

We are IntechOpen, the world's leading publisher of Open Access books Built by scientists, for scientists

6,900

Open access books available

186,000

International authors and editors

200M

Downloads

Our authors are among the

154

Countries delivered to

TOP 1%

most cited scientists

12.2%

Contributors from top 500 universities



WEB OF SCIENCE™

Selection of our books indexed in the Book Citation Index
in Web of Science™ Core Collection (BKCI)

Interested in publishing with us?
Contact book.department@intechopen.com

Numbers displayed above are based on latest data collected.
For more information visit www.intechopen.com



Wind Tunnels in Engineering Education

Josué Njock Libii

Indiana University-Purdue University Fort Wayne

USA

1. Introduction

The subject of fluid mechanics is filled with abstract concepts, mathematical methods, and results. Historically, it has been a challenging subject for students, undergraduate and graduate. In most institutions, the introductory course in fluid mechanics is accompanied by a laboratory course. While institutional philosophy and orientation vary around the world, the goal of that laboratory is to strengthen students' understanding of fluid mechanics using a variety of laboratory exercises (Feisel & Rosa, 2005).

The literature has identified six basic functions of experimental work. Indeed, the report of the Laboratory Development Committee of the Commission on Engineering Education identified six key functions and objectives of the instructional laboratory (Ernest, 1983):

- a. Familiarization
- b. Model identification
- c. Validation of assumptions
- d. Prediction of the performance of complex systems
- e. Testing for compliance with specifications
- f. And exploration for new fundamental information.

The report states that "The role of the undergraduate instructional laboratory is to teach student engineers to perform these six functions. Hence the primary goal of undergraduate laboratories is to inculcate into the student the theory and practice of experimentation. This includes instrumentation and measurement theory." (Ernst, 1983).

The wind tunnel is one such instrument. This chapter focuses on the measurement theory on which the wind tunnel is based and presents examples of its use in the undergraduate fluid mechanics laboratory at Indiana University-Purdue University Fort Wayne, Fort Wayne, Indiana, USA.

The remainder of the chapter is organized in the following manner:

1. *Basic concepts* discuss definitions, classifications, and various uses of wind tunnels.
2. *Fundamental Equations* present the equations that are used as foundations for the theory and application of wind tunnels.
3. *Applications of wind tunnels in teaching fluid mechanics* present nine different examples that are used in our laboratory to teach various aspects of fluid mechanics and its uses in design, testing, model verification, and research.
4. *References* list all cited works in alphabetical order.

2. Basic concepts

2.1 Definition of a wind tunnel

A wind tunnel is a specially designed and protected space into which air is drawn, or blown, by mechanical means in order to achieve a specified speed and predetermined flow pattern at a given instant. The flow so achieved can be observed from outside the wind tunnel through transparent windows that enclose the test section and flow characteristics are measurable using specialized instruments. An object, such as a model, or some full-scale engineering structure, typically a vehicle, or part of it, can be immersed into the established flow, thereby disturbing it. The objectives of the immersion include being able to simulate, visualize, observe, and/or measure how the flow around the immersed object affects the immersed object.

2.2 Classifications of wind tunnels

Wind tunnels can be classified using four different criteria. Four such criteria are presented.

2.2.1 Type 1 classification – The criterion for classification is the path followed by the drawn air: Open- vs. closed-circuit wind tunnels

Open-circuit (open-return) wind tunnel. If the air is drawn directly from the surroundings into the wind tunnel and rejected back into the surroundings, the wind tunnel is said to have an open-air circuit. A diagram of such a wind tunnel is shown in Figure 1.

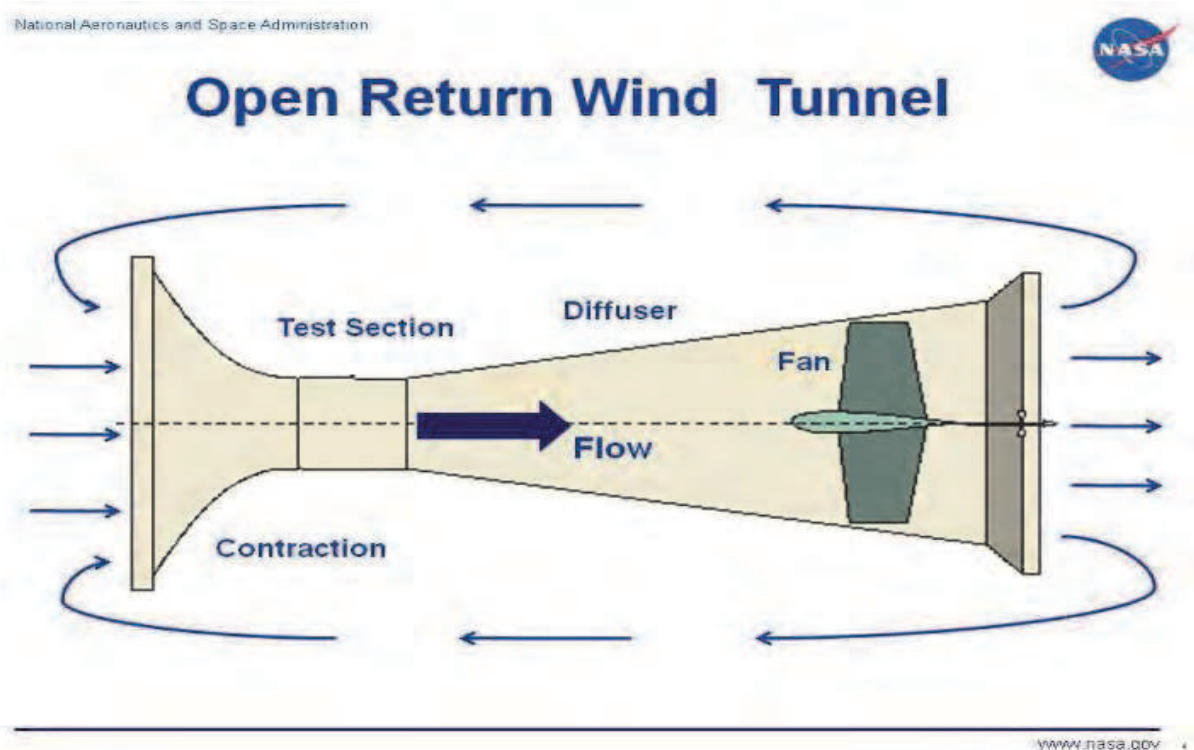


Fig. 1. Diagram of an open-circuit, also known as open-return, wind tunnel (from NASA)

An open-circuit wind tunnel is also called an open-return wind tunnel.

Closed-circuit, or closed-return, wind tunnel. If the same air is being circulated in such a way that the wind tunnel does neither draw new air from the surrounding, nor return it into

the surroundings, the wind tunnel is said to have a closed-air circuit. It is conventional to call that a closed-circuit (closed-return) wind tunnel. Figure 2 illustrates this configuration.

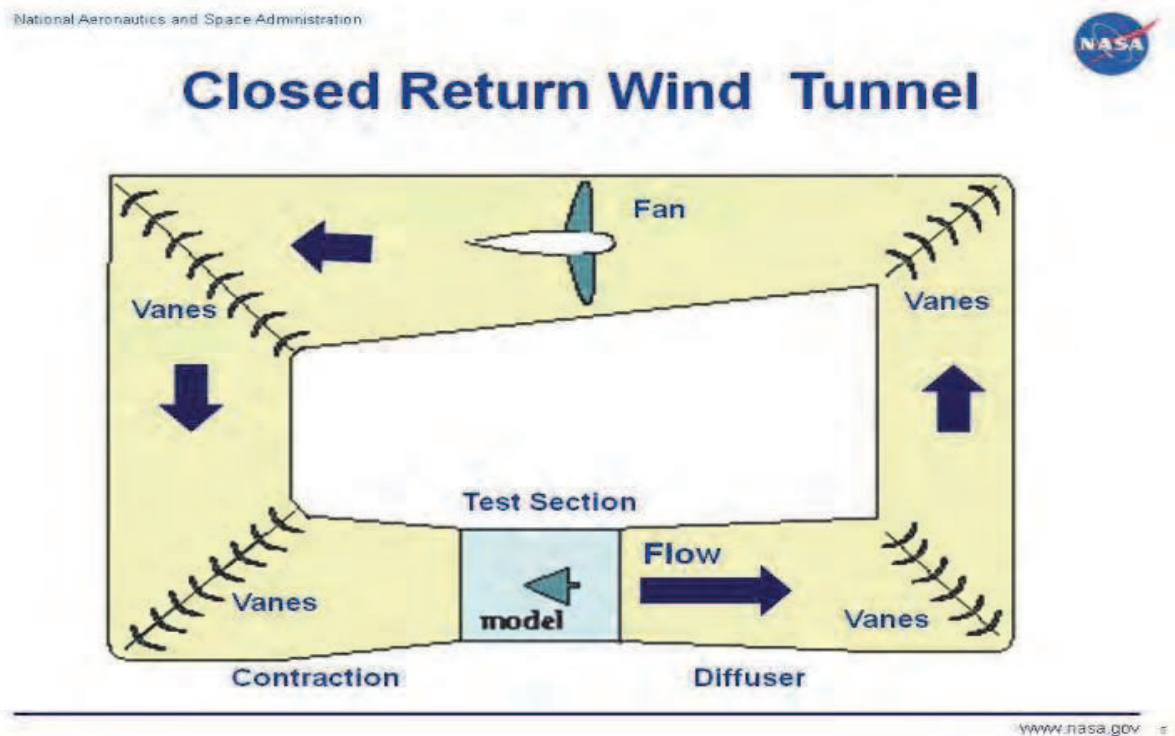


Fig. 2. Top view of a closed-circuit, also known as closed-return, wind tunnel (NASA)

2.2.2 Type 2 classification

The criterion for classification is the maximum speed achieved by the wind tunnel: subsonic vs. supersonic wind tunnels. It is traditional to use the ratio of the speed of the fluid, or of any other object, and the speed of sound. That ratio is called the Mach number, named after Ernst Mach, the 19th century physicist. The classification is summarized in Table 1. Schematic designs of subsonic and supersonic wind tunnels are compared in Figure 3.

Subsonic wind tunnels. If the maximum speed achieved by the wind tunnel is less than the speed of sound in air, it is called a subsonic wind tunnel. The speed of sound in air at room temperature is approximately 343 m/s, or 1235 km/hr, or 767 mile/hr. The Mach number, $M < 1$.

Supersonic wind tunnels. If the maximum speed achieved by the wind tunnel is equal to or greater than the speed of sound in air, it is called a supersonic wind tunnel.

Range of the Mach number , M	Name of flow , or conditions
$M < 1$	Subsonic
$M = 1$, or near 1	Transonic
$1 < M < 3$	Supersonic
$3 < M < 5$	High supersonic
$M > 5$	Hypersonic
$M \gg 5$	High Hypersonic

Table 1. Classification of flows based upon their Mach numbers.



Wind Tunnel Design

Glenn
Research
Center

Increase in Area :

For subsonic flow ($M < 1$)
velocity decreases & pressure increases

For supersonic flow ($M > 1$)
velocity increases & pressure decreases

M = Mach
V = velocity
p = pressure
A = area

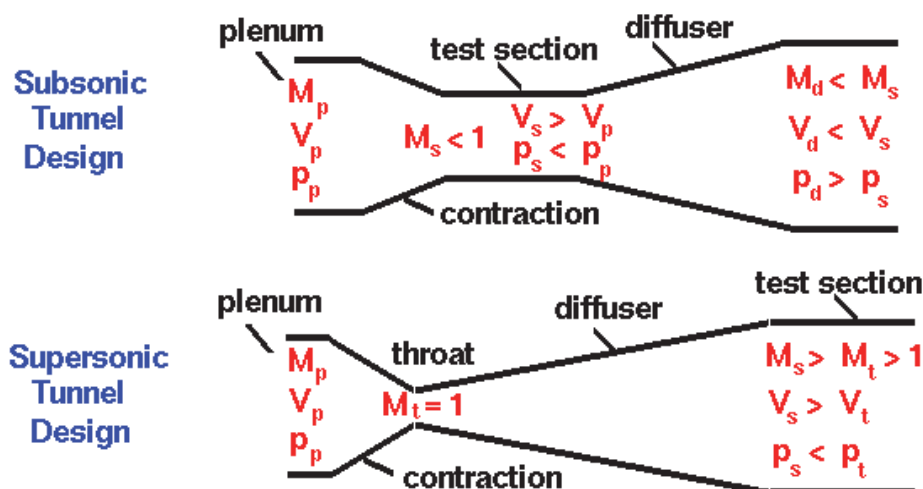


Fig. 3. Schematic designs of subsonic and supersonic wind tunnels (NASA).

2.2.3 Type 3 classification

The criterion for classification is the purpose for which the wind tunnel is designed: research or education. If the wind tunnel is for research it is called a research wind tunnel. If however, it is designed to be used for education, then, it is called an educational wind tunnel.

2.2.4 Type 4 classification

The criterion for classification is the nature of the flow: laminar vs. turbulent flow. Boundary-layer wind tunnels are used to simulate turbulent flow near and around engineering and manmade structures.

2.3 Uses of wind tunnels

There are many uses of wind tunnels. They vary from ordinary to special: these include uses for Subsonic, supersonic and hypersonic studies of flight; for propulsion and icing research; for the testing of models and full-scale structures, etc. Some common uses are presented below. Wind tunnels are used for the following:

2.3.1 To determine aerodynamic loads

Wind tunnels are used to determine aerodynamic loads on the immersed structure. The loads could be static forces and moments or dynamic forces and moments. Examples are

forces and moments on airplane wings, airfoils, and tall buildings. A close-up view of a model of an F-5 fighter plane mounted in the test section of a wind tunnel is shown in Figure 4.

2.3.2 To study how to improve energy consumption by automobiles

They can also be used on automobiles to measure drag forces with a view to reducing the power required to move the vehicle on roads and highways.

2.3.3 To study flow patterns

To understand and visualize flow patterns near, and around, engineering structures. For example, how the wind affects flow around tall structures such as sky scrapers, factory chimneys, bridges, fences, groups of buildings, etc. How exhaust gases ejected by factories, laboratories, and hospitals get dispersed in their environments.

2.3.4 Other uses include

To teach applied fluid mechanics, demonstrate how mathematical models compare to experimental results, demonstrate flow patterns, and learn and practice the use of instruments in measuring flow characteristics such as velocity, pressures, and torques.

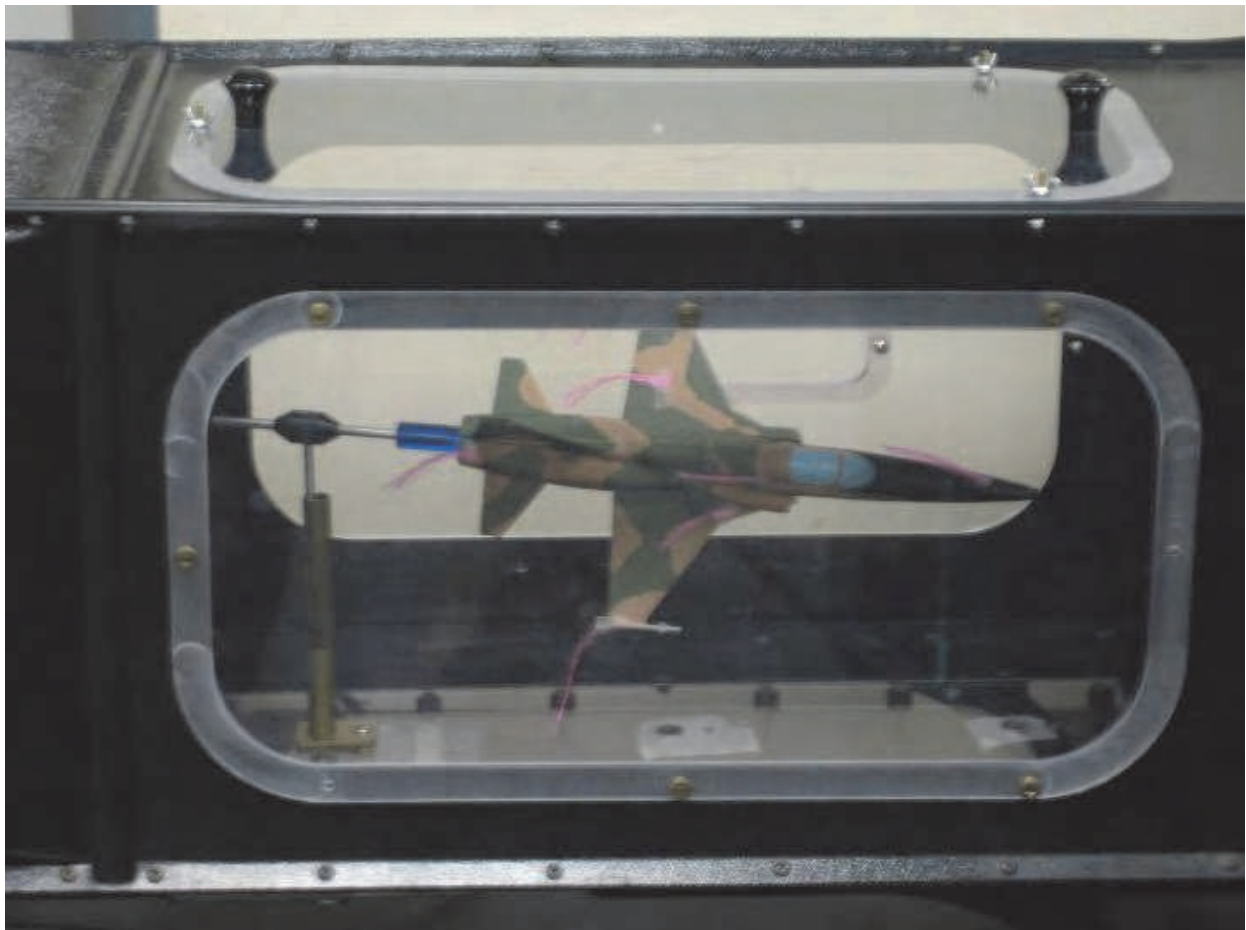


Fig. 4. Close-up of a tufted model of an F-5 fighter plane in the test section of a wind tunnel (NASA)

3. Fundamental equation for flow measurement

Velocity from pressure measurements. One very important use of wind tunnels is to visualize flow patterns and measure the pressure at a selected point in the flow field and compute the corresponding speed of air. The major equation used for this purpose is Eq.(1). It relates the speed of the fluid at a point to both the mass density of the fluid and the pressures at the same point in the flow field. For steady flow of an incompressible fluid for which viscosity can be neglected, the fundamental equation has the form

$$V = \sqrt{\frac{2(p_0 - p)}{\rho}} \quad (1)$$

Where V is the speed of the fluid, P_0 is the total, also called the stagnation, pressure at that point of measurement, and p is the static pressure at the same point. This equation comes from the application of Bernoulli's equation for the steady flow of an incompressible and inviscid fluid along a streamline. Bernoulli's equation is typically obtained by integrating Euler's equations along a streamline. It will be recalled that Euler's equations are a special case of the Navier-Stokes equations, when the viscosity of the fluid has been neglected. The Navier-Stokes' equations, in turn, are obtained from Newton's second law when it is applied to a fluid for which the shear deformation follows Newton's law of viscosity. Accordingly, in order to establish the theoretical validity of this equation for use in educational wind tunnels, it is important to review some basic results from the theory of viscous and inviscid flows. For the interested reader, these are available in all introductory textbooks of fluid mechanics (e.g. Pritchard, 2011). For this reason, the rest of this chapter will emphasize applications of the results of fluid mechanics theory as they pertain to the use of wind tunnels for instructional purposes.

4. Applications of wind tunnels in teaching fluid mechanics

This section discusses nine different laboratory exercises in which the wind tunnel is used to measure fluid flow parameters. They are: 1) measurement of air speed; 2) verification of the existence of the boundary layer over a flat plate; 3) determination and characterization of the boundary layer over a flat plate; 4) searching for evidence of turbulence in boundary layer flow; 5) measurement of pressure distributions around a circular cylinder in cross flow; 6) determination of the viscous wake behind a circular cylinder in cross flow; 7) determination of lift and drag forces around airfoils; 8) reduction of drag by the introduction of turbulence in the boundary layer; and 9) determination of the Richardson's annular effect in flow through a duct.

4.1 Measurement of air speed using an open-circuit wind tunnel

4.1.1 Purpose

The purpose of this experiment is to learn how to use the wind tunnel to measure the difference between the stagnation (total) pressure and the static pressure at a specific point of a flow field and use that difference to compute the wind speed at that point using Bernoulli's equation.

4.1.2 Key equation

The key equation is

$$V = \sqrt{\frac{2(p_0 - p)}{\rho}} \quad (1)$$

4.1.3 Experimental procedure

The experimental procedure consists of four steps:

1. Read the temperature and the pressure inside the lab, or inside the wind tunnel, or both.
2. Use these values to compute the mass density of air inside the lab using the ideal gas law. Or use these values to look up the mass density of air on a Table.
3. Use the wind tunnel to measure the pressure difference, $p_0 - p$, at the point of interest.
4. Use Eq. (1) to compute the speed of the air at that point.

A sketch of the open-circuit wind tunnel used in our lab is shown below. It is a subsonic wind tunnel that is equipped with static- and dynamic-pressure taps, a pressure-sensing electronic device (See Figure 5).

In this setup, the stagnation pressure is measured by the pressure probe, while the static pressure is measured using a wall tap. This is illustrated graphically in Figure 6(a).

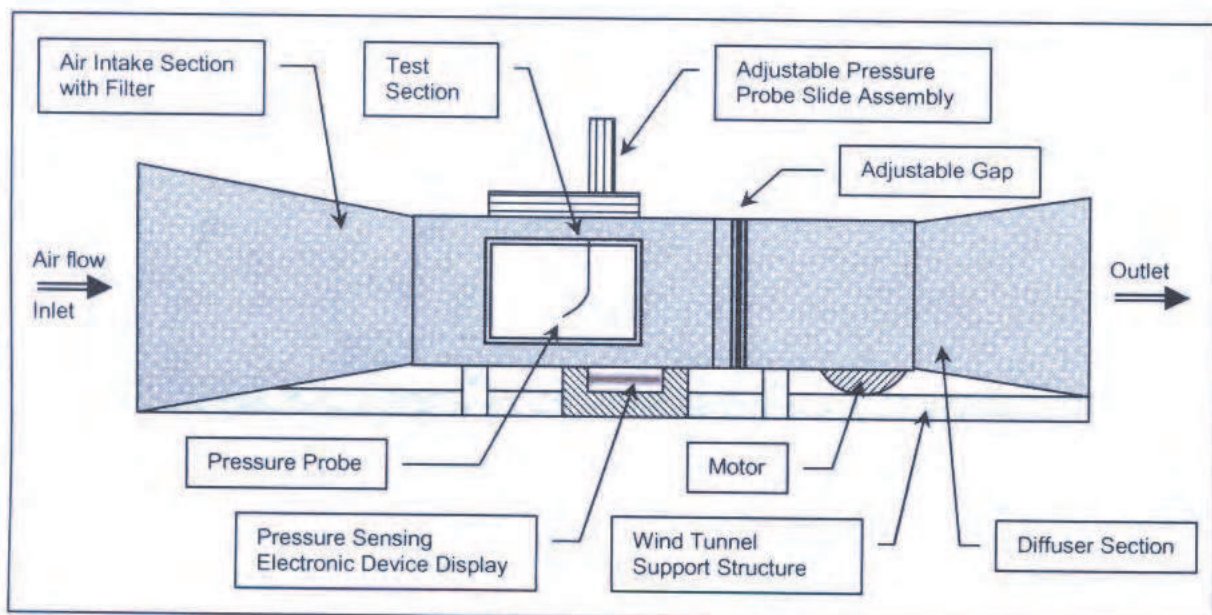


Fig. 5. Sketch of the wind tunnel used (Courtesy of Joseph Thomas, 2006)

Students often wonder whether or not the use of a wall tap is correct; that is, if it can be justified using analysis. And the answer is that it is and it can. The use of a wall tap is allowable because the flow is presumed, and is in fact, essentially parallel. An illustration of parallel flow is shown in Figure 7.

Under parallel-flow conditions, Eq.(2), which is Euler's equation, written along a coordinate axis that is normal to the local streamline, indicates that the curvature of the local streamlines is extremely large, which causes the pressure gradient in the direction perpendicular to the streamlines to be zero, making the pressure constant in the direction

normal to the streamline. Therefore, the value of the static pressure measured by the wall tap is the same as that which would have been measured at the tip of the stagnation probe.

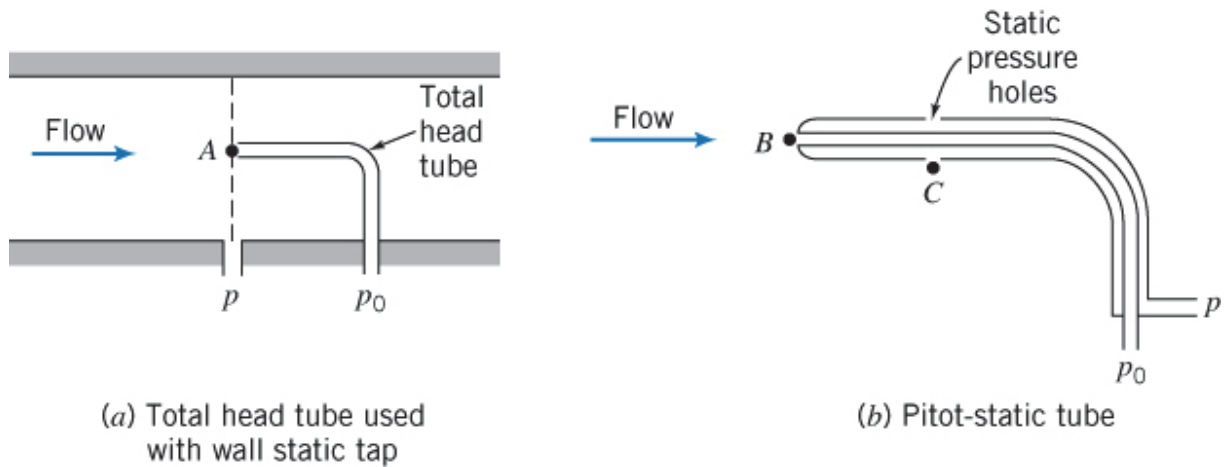


Fig. 6. Two different ways to measure the total and static pressures inside the test section (Pritchard, 2011).

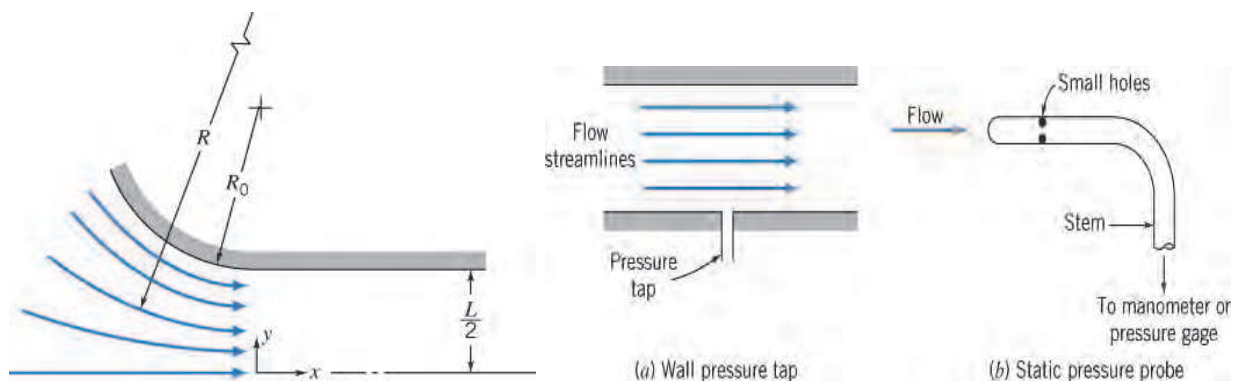


Fig. 7. Illustration showing that the radius of curvature becomes very large inside the test section (Pritchard, 2011).

$$\rho \left(\frac{V^2}{R} \right) = \frac{\partial p}{\partial n} \Rightarrow \frac{1}{\rho} \frac{\partial p}{\partial n} = \frac{V^2}{R}; \quad (2)$$

Parallel - flow $\Rightarrow R \rightarrow \infty, \frac{\partial p}{\partial n} \rightarrow 0$

4.1.4 Experimental results

The speed in the test section can be changed by increasing, or decreasing, the air gap between the diffuser section and the intake section of the wind tunnel (Fig. 5). When the air gap is completely closed, the speed in the test section is at its maximum value; when it is as large as possible, the speed in the test section is at its minimum. By starting with the gap completely closed, opening it by very small increments, and measuring the speed of air at each step, one gets a calibration curve that relates the speed in the test section to the size of the air gap. A sample curve obtained after executing this procedure in our wind tunnel is shown below (Njock Libii, 2006).

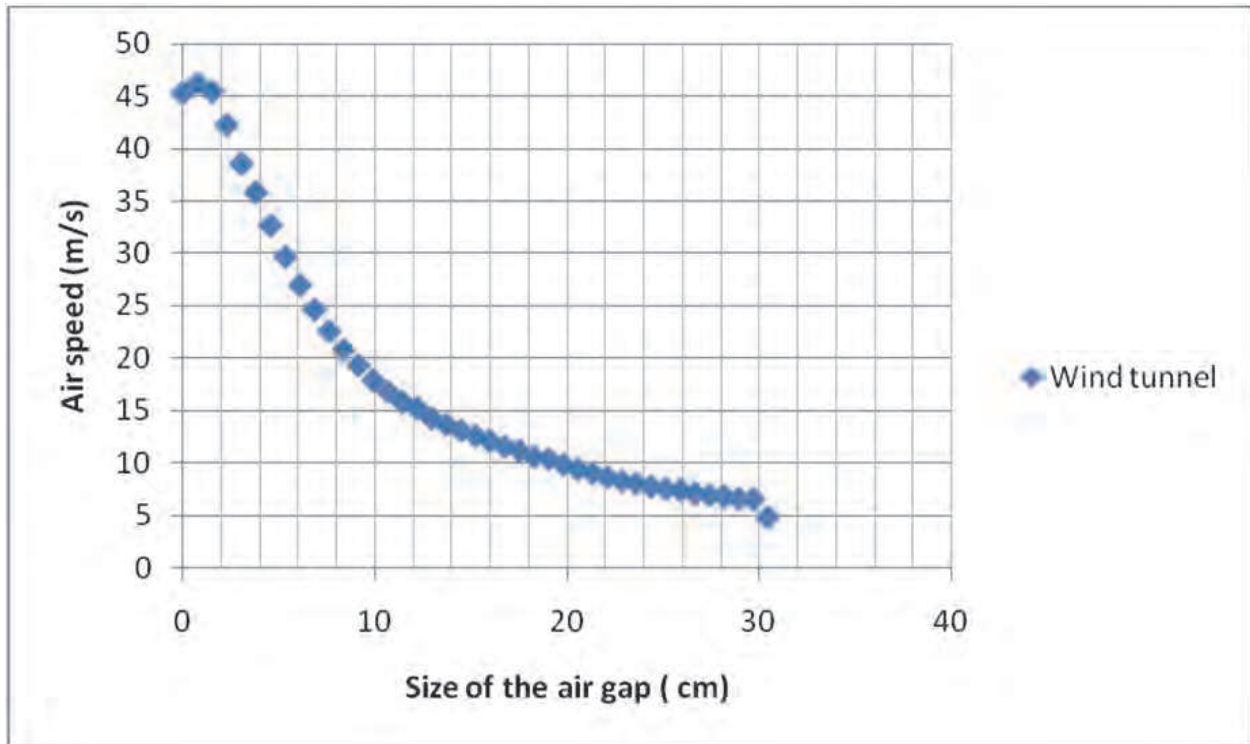


Fig. 8. Variation of wind speed in the test section with the size of the air gap.

4.2 Experimental verification of the existence of the boundary layer over a flat plate

4.2.1 Purpose

The purpose of this experiment is to learn how to use the wind tunnel to measure the difference between the stagnation (total) pressure and the static pressure at a series of points located on a vertical line selected in the flow field and use those differences to compute the wind speeds at each such point using Bernoulli's equation. The plotting of the resulting velocity profile and its examination will be used to determine whether or not the existence of the boundary layer can be detected.

Many viscous flows past solid bodies can be analyzed by dividing the flow region into two subregions: one that is adjacent to the body and the other that covers the rest of the flow field. The influence of viscosity is concentrated, and only important, in the first subregion, that which is adjacent to the body. The effects of viscosity can be neglected in the second subregion, that is, outside of the region adjacent to the body. The first region has been called the boundary layer historically. This phrase is a translation of the German phrase used by Prandtl, who introduced this concept. A big problem in fluid mechanics is locating the line that demarcates the boundary between the two subregions. Locating this line is also called determination of the boundary layer, or simply the boundary-layer problem.

The symbol used for the local thickness of this boundary layer is δ . It denotes the distance between a point on the solid body and the point beyond which the effect of viscosity can be considered to be negligible.

4.2.2 Key equations

Thickness of the laminar boundary layer over a flat plate: Exact solution due to Blasius. For a semi-infinite flat plate, the exact solution for a laminar boundary layer was first derived by

Blasius (Pritchard, 2011). In conformity with his work, the continuity equation and the Navier-Stokes equation with the corresponding boundary conditions are ordinarily written as shown below:

$$\begin{aligned} \frac{\partial u}{\partial x} + \frac{\partial v}{\partial y} &= 0 \\ u \frac{\partial u}{\partial x} + v \frac{\partial u}{\partial y} &= \nu \frac{\partial^2 u}{\partial y^2} \\ u(y=0) &= 0; v(y=0) = 0 \\ u(y=\infty) &= U; \frac{\partial u}{\partial y}(y=\infty) = 0 \end{aligned} \quad (3)$$

Where u is the component of velocity along the plate and v is the component of velocity perpendicular the plate. The origin of the coordinate system is at the leading edge of the plate, with the x direction along the plate and the y direction perpendicular to it. The magnitude of free-stream velocity, far from the plate is U .

Using similarity transformations, one introduces a change of variables as shown below. Let

$$\begin{aligned} \eta &\propto \frac{y}{\delta} \Rightarrow \frac{u}{U} = g(\eta); \\ \delta &\propto \sqrt{\frac{\nu x}{U}} \Rightarrow \eta = y \sqrt{\frac{U}{\nu x}} \\ u &= \frac{\partial \psi}{\partial y}; v = -\frac{\partial \psi}{\partial x}; f(\eta) = \frac{\psi}{\sqrt{\nu x U}} \end{aligned} \quad (4)$$

Applying this change of variables allows the second-order partial differential equation given above to become a nonlinear, third-order, ordinary differential equation, with the associated boundary conditions shown below:

$$\begin{aligned} 2 \frac{d^3 f}{d\eta^3} + f \frac{d^2 f}{d\eta^2} \\ f(\eta=0) &= 0; \frac{df}{d\eta}(\eta=0) = 0 \\ \frac{df}{d\eta}(\eta \rightarrow \infty) &= 1. \end{aligned} \quad (5)$$

The solution to this equation is obtained numerically. From that numerical solution, it is seen that, at $\eta = 5.0$, $u/U = 0.992$. If the boundary layer thickness is defined as the value of y for which $u/U = 0.99$, one gets

$$\delta \cong \frac{5.0x}{\sqrt{\text{Re}_x}}; \text{with } \text{Re}_x = \frac{Ux}{\nu} \quad (6)$$

Using boundary-layer theory, a sketch of the velocity profile along a vertical line in the test section of the wind tunnel is expected to look as shown below. In this application of the

wind tunnel, one wishes to compare this profile to that obtained experimentally in the test section of the wind tunnel (See Figure 9.).

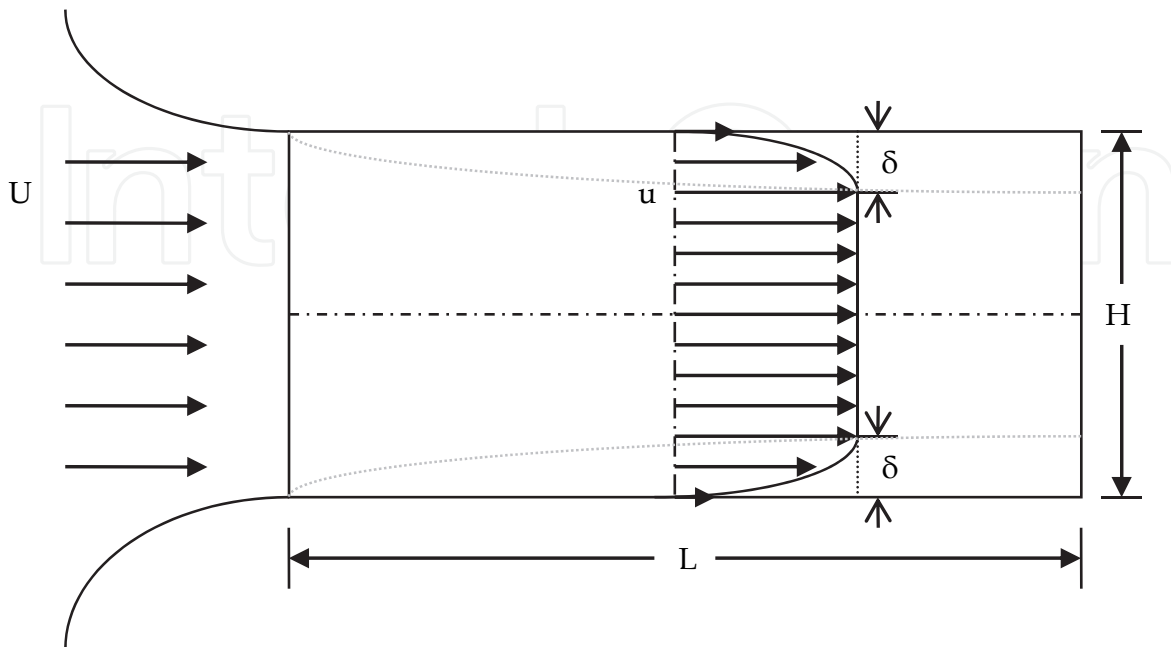


Fig. 9. Graphical Representation of Boundary Layer Theory in Wind Tunnel Test Section

4.2.3 Experimental procedure

The experimental procedure consists of the following steps:

1. Choose a vertical plane in the test section.
2. Choose a vertical line within that vertical plane.
3. Select a series of points along that vertical line where the velocity of the air will be determined.
4. Read the temperature and the pressure inside the lab, or inside the wind tunnel, or both.
5. Use these values to compute the mass density of air inside the lab using the ideal gas law. Or Use these values to look up the mass density of air on a Table.
6. Select a wind speed and set the wind tunnel to generate that wind speed inside the test section.
7. Use the wind tunnel at that set speed to measure the pressure difference, $p_0 - p$, at each point that was identified along the preselected vertical line. This process is known as traversing a cross section of the flow space.
8. Use Eq. (1) to compute the speed of the air at each such point.

4.2.4 Experimental results

A sample curve obtained after executing this procedure in our wind tunnel is shown below (Njock Libii, 2010). The wind speed was set at 46 m/s, approximately. By comparing Fig. (9) and Fig. (10), it can be concluded that experimental data clearly show the existence of the boundary layer. Note. Because the tip of the probe had a finite thickness (of 5 mm), students could not get infinitely close to the wall in measuring the speed of air in the wind tunnel (Njock Libii, 2010).

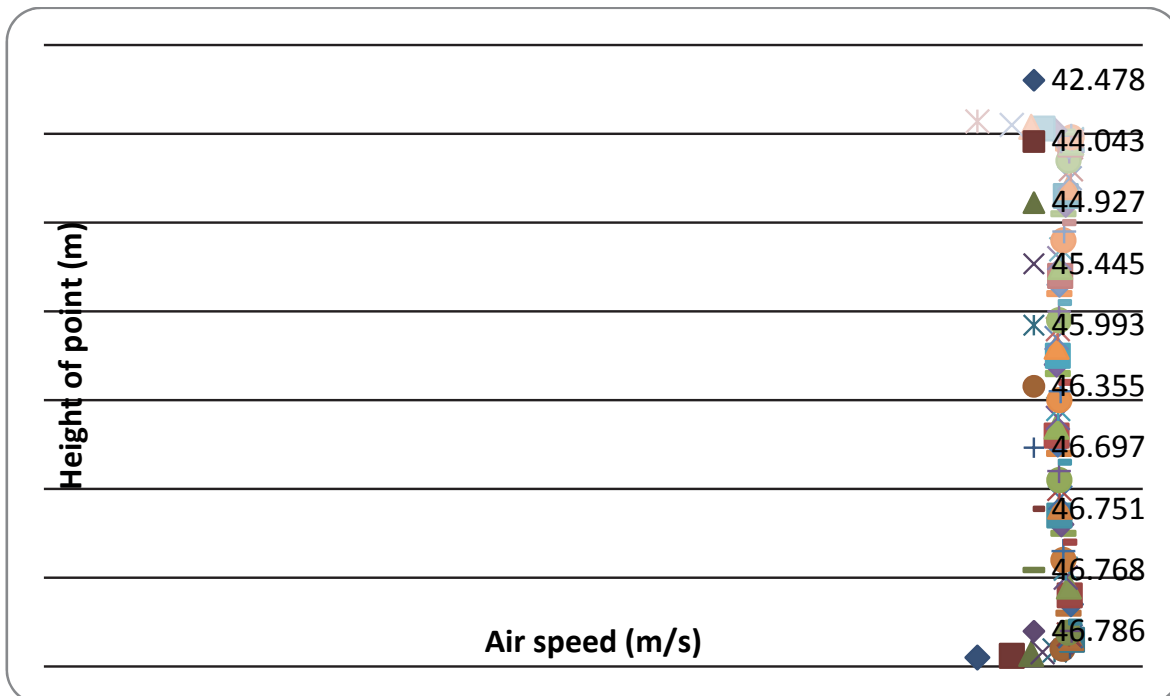


Fig. 10. Experimental velocity profile of the flow in the test section for a speed of 46 m/s

4.3 Determination and characterization of the boundary layer along a flat plate

4.3.1 Purpose

The purpose of this experiment is to learn how to use experimental data collected in a wind tunnel to determine the thickness of the boundary layer and to characterize the type of boundary layer that is represented by such data.

4.3.2 Key equations

The boundary layer over a flat plate can be laminar, turbulent, or transitional, meaning that it is somewhere between laminar and turbulent. Whether boundary layer is laminar or turbulent depends upon the magnitude of the Reynolds of the flow. Such a Reynolds number is defined as shown in Eq.(7),

$$Re_x = \frac{Ux}{\nu} \quad (7)$$

Where U is the freestream velocity, ν is the kinematic viscosity, and x is the distance from the leading edge of the plate to some point of interest. By convention, a boundary player becomes turbulent when the Reynolds number of the flow exceeds 5×10^5 .

For flow inside the test section, where, instead of inserting a plate, it is the bottom surface of the test section that takes the role of the flat plate, the location of the leading edge of the plate must be estimated. In the case of the data reported here, it was estimated in the following way: the leading edge was defined as the line where the curved section that constitutes the intake of the tunnel becomes horizontal, and hence, tangential to the inlet to the test section. In the wind tunnel used for these tests, that line was at a distance of $0.356 \text{ m} < x < 0.457 \text{ m}$ from the plane that passes through the geometric center (centroid) of the test section. The free stream speed was $U = 46 \text{ m/s}$; and using a kinematic viscosity of $15.68 \times$

10^{-6} m²/s, corresponding to a room temperature of (20^o C) on the day of the experiment, the Reynolds number was found to be

$$1.05 \times 10^6 < \text{Re}_x = \frac{Ux}{\nu} < 1.40 \times 10^6 \quad (8)$$

From these results, $5 \times 10^5 < 1.05 \times 10^6 < \text{Re}_x = \frac{Ux}{\nu} < 1.40 \times 10^6$, and the boundary layer is turbulent. Therefore, the boundary layer thickness given by the Blasius solution is not applicable. Instead, one can use the momentum- integral equation to estimate the thickness of the boundary layer. That equation is given by

$$\frac{\tau_w}{\rho} = \frac{d}{dx}(U^2\theta) + \delta^*U \frac{dU}{dx} \quad (9)$$

Where τ_w is the shear stress at the wall, θ is the momentum thickness, and δ^* is the displacement thickness. These are defined as follows:

The displacement thickness: δ^*

$$\delta^* = \int_0^\infty \left(1 - \frac{u}{U}\right) dy = \int_0^\delta \left(1 - \frac{u}{U}\right) dy \quad (10)$$

The momentum thickness: θ

$$\theta = \int_0^\infty \frac{u}{U} \left(1 - \frac{u}{U}\right) dy = \int_0^\delta \frac{u}{U} \left(1 - \frac{u}{U}\right) dy \quad (11)$$

And the boundary-layer thickness is δ .

Since the expression for the flow inside the boundary layer is not known, one uses the power-law formula for pipe flow but adjusted to boundary layer flows. It is

$$\frac{u}{U} = \left(\frac{y}{\delta}\right)^{1/n} = \eta^{1/n} \quad (12)$$

Where n is unknown. Using different values of n allows one to construct a Table such as the one shown below (Njock Libii, 2010).

$\frac{u}{U} = \eta^{1/n}$	$\frac{\theta}{\delta}$	$\frac{\delta^*}{\delta}$	$H = \frac{\delta^*}{\theta}$	$a \equiv \frac{\delta}{x} (\text{Re}_x)^{1/5}$	$b = C_f (\text{Re}_x)^{1/5}$
$\eta^{1/6}$	0.107143	0.142857	1.333333	0.337345906	0.057830727
$\eta^{1/7}$	0.097222	0.125	1.285714	0.381143751	0.059289028
$\eta^{1/8}$	0.088889	0.111111	1.250000	0.423532215	0.060235693
$\eta^{1/9}$	0.0818181	0.100000	1.222222	0.464755563	0.060840728
$\eta^{1/10}$	0.0757575	0.9090909	1.200000	0.504990077	0.061210918

Table 2. Turbulent boundary layer over a flat plate at zero incidence: results

For the case of $n = 7$, one has

$$\frac{u}{U} = \left(\frac{y}{\delta}\right)^{1/7} = \eta^{1/7} \quad (13)$$

The boundary layer thickness is then given by

$$\delta \cong \frac{0.382x}{(\text{Re}_x)^{1/5}}; \text{with } \text{Re}_x = \frac{Ux}{\nu} \quad (14)$$

In the case tested here, where $U = 46 \text{ m/s}$, $0.356 \text{ m} < x < 0.457 \text{ m}$, and for which $1.05 \times 10^6 < \text{Re}_x = \frac{Ux}{\nu} < 1.40 \times 10^6$, the thickness of the boundary layer is found to be

$$8.5\text{mm} < \delta < 10.4\text{mm} \quad (15)$$

4.3.3 Experimental procedure

Using the data shown in Fig. 10, the boundary layer thickness can be estimated by extracting the y coordinate of the point where the velocity profile begins to turn toward (or, away from) the wall.

4.3.4 Experimental results

Using the data shown in Fig. 10, the boundary layer thickness was estimated by extracting the y coordinate of the point where the velocity profile begins to turn toward (or, away from) the wall. That value is $y = 0.01087 \text{ m} = 10.87 \text{ mm}$. This value is close to the upper bound obtained from theory, Eq.(14), by the power law formula with $n=7$. Using $n = 8$, instead of $n = 7$, however, the theoretical range of thicknesses becomes $9.4\text{mm} < \delta < 11.53\text{mm}$. A comparison Table is shown on Table 3.

n	Thickness from analysis	Thickness from experiment
7	$8.5\text{mm} < \delta < 10.4\text{mm}$	10.87 mm
8	$9.4\text{mm} < \delta < 11.53\text{mm}$	10.87 mm

Table 3. Tabulated comparisons of the thicknesses of turbulent boundary layers

4.4 The existence of turbulence in the flow stream

4.4.1 Purpose

The purpose of this experiment is to learn how to use experimental data collected in a wind tunnel to determine the fluctuations in the air pressure inside the test section.

4.4.2 Key equations

Flow in the test section is presumed to be steady. However, because of the rotation of the fan blades and the vibration in the housing that supports the wind tunnel, fluctuations are introduced in the air stream. Some of these are detectable using pressure measurements.

$$\text{Fluctuation} \equiv \left(\frac{P_{\max} - P_{\min}}{P_{\max}}\right) \times 100 \quad (15a)$$

4.4.3 Experimental procedure

At each point where pressures were measured, each measured pressure fluctuated rapidly between minimum and maximum values. These could be displayed by the pressure sensors. Although it was not done for the data presented, it was also possible, if one wished, to measure the instantaneous fluctuations that occurred.

4.4.4 Experimental results

Figure 11 displays the averaged fluctuations, that is the differences between the maximum and minimum values of pressures at each tested point during the experiment, Eq. (15a). The average fluctuation was around 3 %.

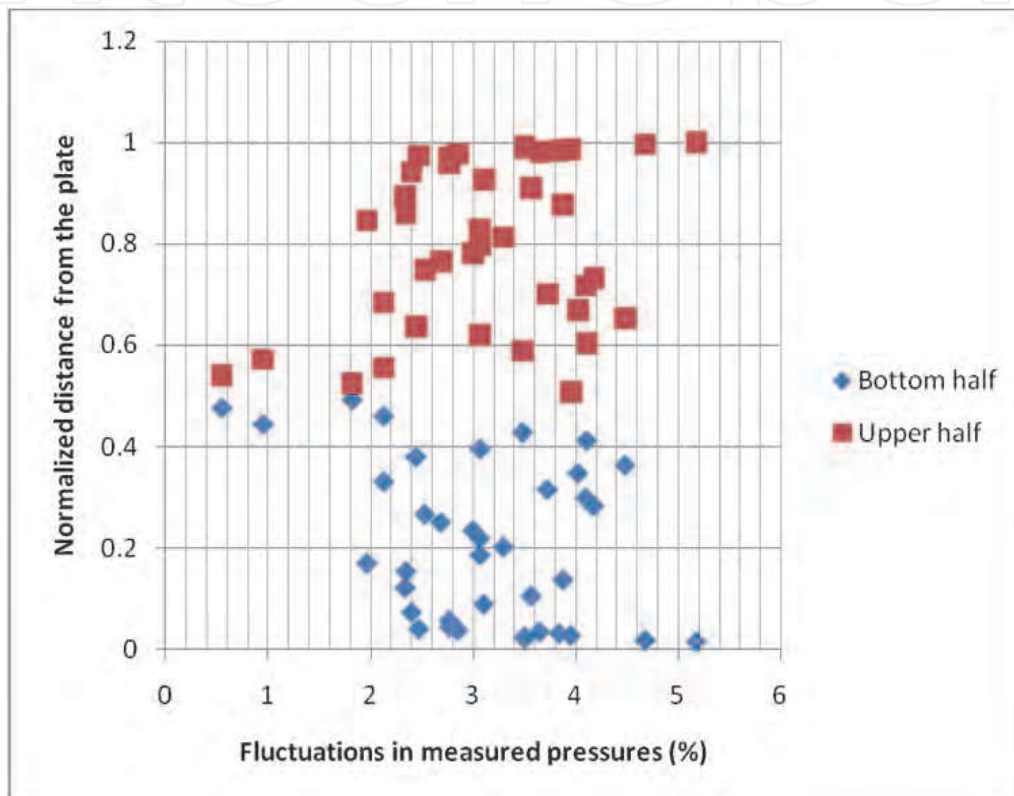


Fig. 11. Pressure fluctuations inside the test section at an air speed of 46 m/s.

4.5 Measuring pressure distributions around a circular cylinder in cross flow

4.5.1 Purpose

The purpose of this laboratory exercise is to measure the pressure distribution on a right circular cylinder and compare the result to those predicted by inviscid-flow theory and to experimental results found in the literature.

4.5.2 Key equations

For steady, frictionless, and incompressible flow from left to right over a stationary circular cylinder of radius "a" the velocity is given by

$$\vec{V} = v \left[\left(1 - \frac{a^2}{r^2} \right) \cos \theta \right] \vec{e}_r - v \left[\left(1 + \frac{a^2}{r^2} \right) \sin \theta \right] \vec{e}_\theta \quad (16)$$

Using Bernoulli's equation, the pressure distribution on the surface of the cylinder is found to be

$$\frac{P_c - P_\infty}{\rho} = \frac{v^2}{2} (1 - 4 \sin^2 \theta) \quad (17)$$

from which the pressure coefficient, C_p , can be deduced. Thus,

$$C_p = \frac{P_c - P_\infty}{\frac{1}{2} \rho v^2} = 1 - 4 \sin^2 \theta \quad (18)$$

Unfortunately, an expression of C_p vs. θ similar to the one in equation (18) cannot be obtained analytically for the steady flow of an incompressible viscous fluid. However, one can obtain experimental data by measuring the pressure on the surface of the cylinder as a function of the position, θ . Such data can be plotted and compared with the graph of equation (18). Generating such a plot is the purpose of this lab.

Such plots are available in the literature and in almost all textbooks of fluid mechanics.

4.5.3 Experimental procedure

A wind tunnel is used so that students can collect their own data and generate these curves themselves. This can be done, say, by following the procedure shown below:

1. Install the cylinder inside the wind tunnel and connect it to the pressure tap.
2. Set the speed in the tunnel to the desired value
3. Measure the pressure on the surface of the cylinder for angles of rotation from 0° to 360° , in 10° increments. Perform the rotations in both the clockwise and counterclockwise directions. Record the measurements at each station.

4.5.4 Experimental results

A wind tunnel has been used; students collected their own data and generated curves similar to those shown below by themselves. Sample results are shown in reference cited below. This conceptual approach was implemented in our laboratory and the collected data verified what is reported in the literature (Njock Libii, 2010).

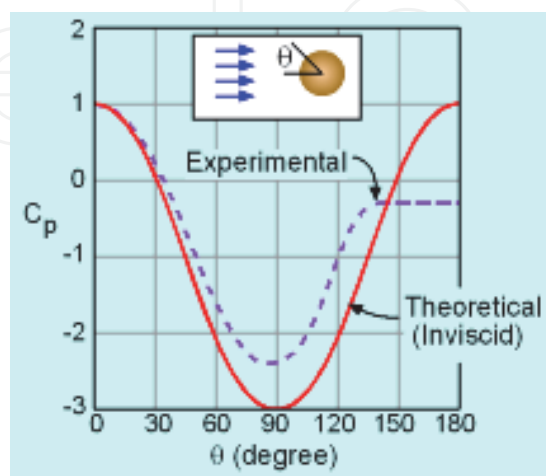


Fig. 12. Comparison of C_p for: inviscid and viscous flows (Pritchard, 2011).

4.6 Experimental determination of the viscous wake behind a circular cylinder

4.6.1 Purpose

The purpose of this laboratory exercise is to use the pressure probe to measure the pressure behind a right circular cylinder and use the results to estimate the width of the viscous wake behind the circular cylinder. Then, compare the results to those predicted by inviscid-flow theory.

4.6.2 Key equations

When flow is inviscid, there is no flow separation and, therefore, no viscous wake. The introduction of viscosity allows for flow separation to occur and for the generation of a viscous wake. By sensing the pressure across the wake, students can compare their measured values to those that are expected to occur outside the wake. This allows for the estimation of the width of the wake behind the cylinder.

4.6.3 Experimental procedure

1. Install the cylinder inside the wind tunnel and connect it to the pressure tap.
2. Set the speed in the tunnel to the desired value.
3. Choose a distance that is two diameters away and upstream from the leading edge of the cylinder.
4. Measure the pressure at that section. This pressure will be used as a reference pressure.
5. Identify and mark ten preselected sections behind the cylinder. Use the following distances: d , $2d$, $3d$, $4d$, $5d$, $6d$, $7d$, $8d$, $9d$, and $10d$, where d is the diameter of the cylinder and each distance is measured from the leading edge of the cylinder.
6. Measure the pressure behind the surface of the cylinder at each predetermined section.
7. At each distance, traverse the corresponding vertical cross section of the wake until the pressure registered becomes approximately equal to that which was measured in step 4. Note the points at which this occurred. Measure their vertical distances from the horizontal axis of symmetry of the cylinder.

4.6.4 Experimental results

Plot the points from your experiment that represent the boundary curve that separates the wake from the external flow. This curve estimates the width and length of the viscous wake behind the cylinder. Curves will resemble Fig. 13.

4.7 Experimental determination of lift and drag forces on an airfoil

4.7.1 Purpose

Students measure the lift and drag of several different airfoils using a force balance and a subsonic wind tunnel, and they compare the results to published data and theoretical expectations.

4.7.2 Key equations

The lift coefficient, C_L , is given by

$$C_L = \frac{F_L}{\frac{1}{2}\rho V^2 A} \quad (19)$$

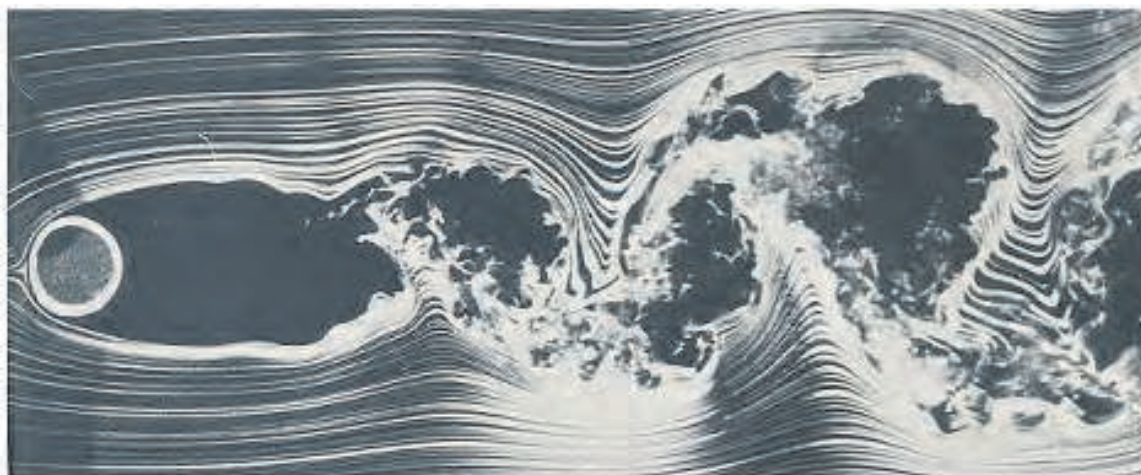
Where F_L is the lift force, V is the average speed, and A is the reference area. The drag coefficient, C_D , is given by

$$C_D = \frac{F_D}{\frac{1}{2}\rho V^2 A} \quad (20)$$

Where F_D is the drag force, V is the average speed, and A is the reference area.

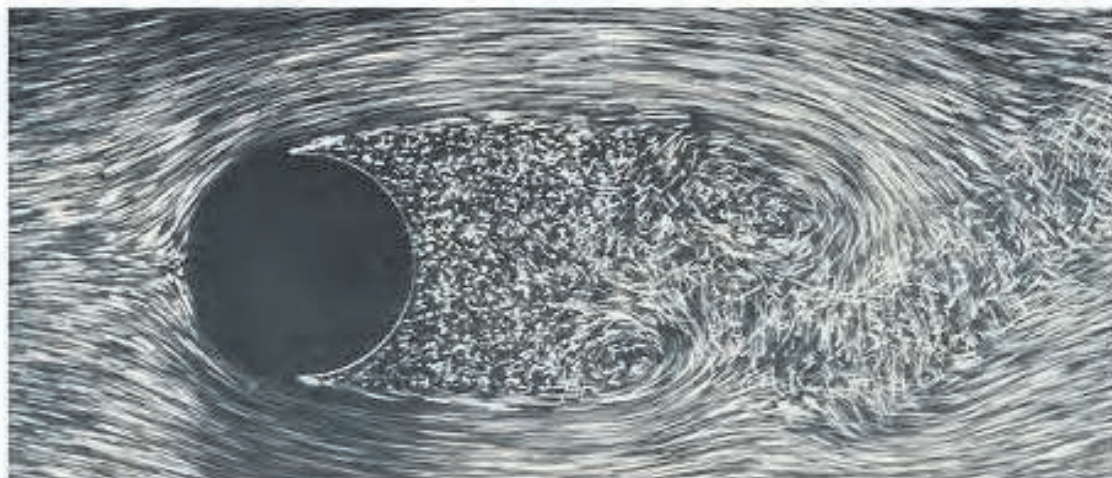
4.7.3 Experimental procedure

With the appropriate equipment one can measure lift and drag on an airfoil in a wind tunnel. Many universities have these setups and corresponding experiments. A particularly nicely presented one is that for a course on Aerospace Engineering Laboratory at Rutgers University (Rutgers, 2011). In that experiment, students measure the lift and drag of several different airfoils using a force balance and subsonic wind tunnel, and they compare the results to published data and theoretical analysis.



(a) Visualizing turbulent cylinder wake at $Re = 10000$

[Courtesy: Thomas Corke and Hassan Nagib; from *An Album of Fluid Motion* by van Dyke (1982)]



(b) a closer look at $Re = 2000$ - patterns are identical as in (a)

[Courtesy: ONERA pic. Werle & Gallon (1972) from *An Album of Fluid Motion* by van Dyke (1982)]

Fig. 13. Experimentally-determined wakes behind a circular cylinder in viscous flow

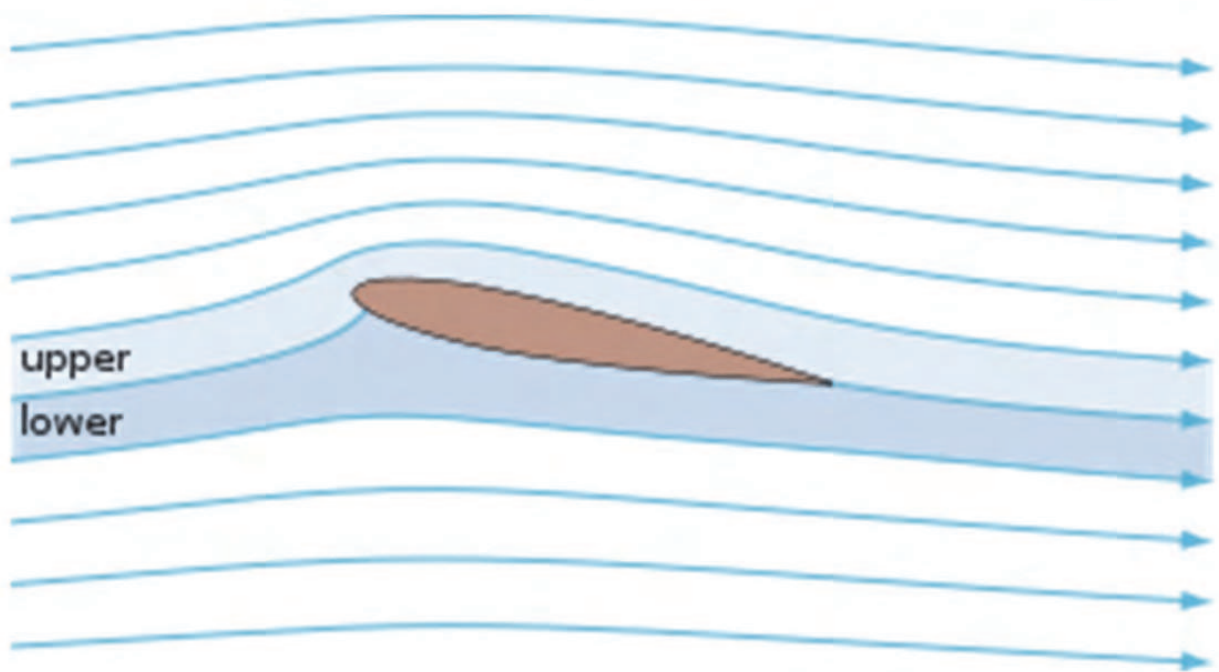


Fig. 14. Streamlines around a NACA 0012 airfoil at a moderate angle of attack.

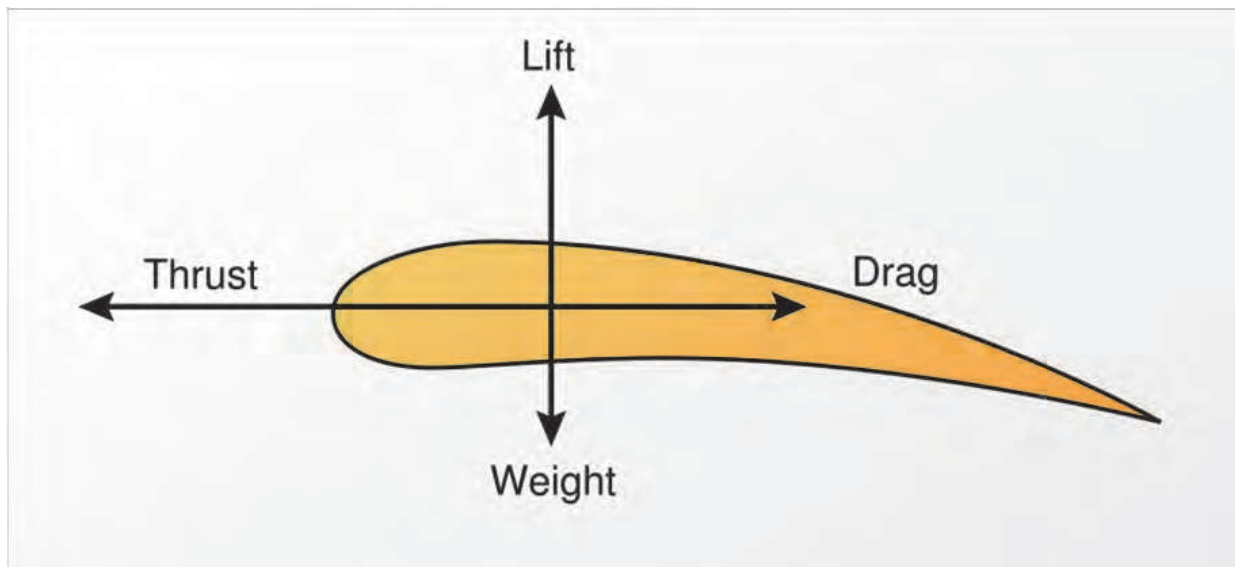


Fig. 15. Schematic representation of lift, drag, thrust, and weight on an airfoil.

4.7.4 Experimental results

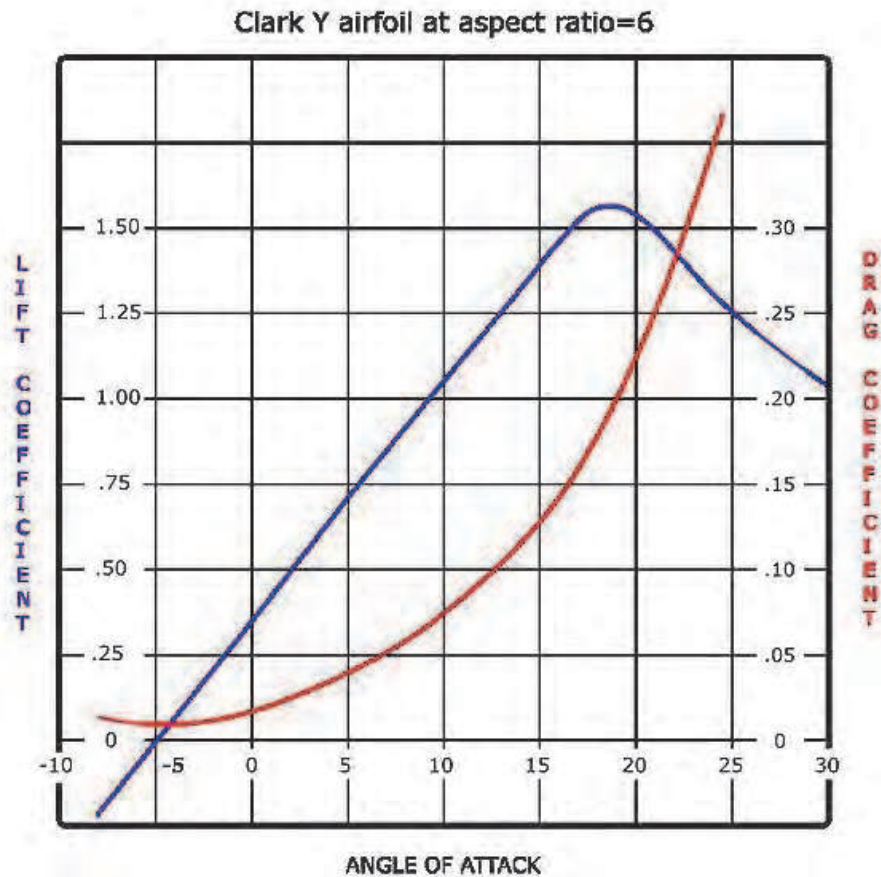


Fig. 16. Sample variation of lift and drag on an airfoil with the angle of attack.

4.8 Reduction of drag by inducing turbulence in the boundary layer

4.8.1 Purpose

The purpose of this laboratory exercise is to measure and compare drag forces exerted on smooth and rough spheres of the same size and use collected data to verify the claim that roughness on the surface of a sphere reduces the drag force on it.

4.8.2 Key equations

The drag coefficient is defined as the ratio obtained by dividing the drag force by the inertial force of the fluid stream, Eq.(20). From this equation, the drag force on a sphere of diameter d is

$$F_D = \frac{(\pi \rho v^2 d^2)}{8} C_D \quad (21)$$

From Eq.(21), if a rough sphere and a smooth sphere of equal diameters are in the same fluid, the differences in their drag forces would be borne by the drag coefficient, C_D .

If a sphere is suspended in the test section of the wind tunnel in such a way as to create a simple pendulum that makes an angle θ with the vertical, and for which the sphere is the

bob, then, neglecting the lift force, the drag force is related to the deflection of the pendulum by

$$F_D = mg \tan \theta \quad (22)$$

Using Eq. (22), the drag force per unit weight becomes

$$\frac{F_D}{mg} = \tan \theta \quad (23)$$

If one uses a rough sphere and a smooth sphere of equal weights, then, the effect of the roughness on the drag force would be borne by the deflection angle.

4.8.3 Experimental procedure

1. Create equal numbers of smooth and rough spheres
2. Make sure that for each smooth sphere, there is a rough sphere of the same size and weight
3. Place each sphere by itself in the fluid stream of the wind tunnel
4. Select a wind speed for the test
5. Measure the drag force on that sphere
6. Repeat this process for each sphere in the whole set
7. Select a set of wind speeds to be used for the test
8. Repeat steps 3 through 6 for each wind speed selected
9. Use collected data to compare the drag forces in each pair
10. Determine whether or not your data allow you to verify the claim that adding roughness to the surface of a sphere reduces the drag force on it.

4.8.4 Experimental results

This conceptual approach was implemented in our laboratory and the collected data verified that roughness on the surface of a sphere reduces the drag force on it. A sample plot of results is shown in Figure 17. The procedures followed to create this experiment are detailed in a paper by the author (Njock Libii, 2006), while the complete set of data and discussion are presented in another paper (Njock Libii, 2007).

4.9 Demonstration of the Richardson's annular effect

4.9.1 Purpose

The purpose of this exercise is to use data obtained from wind tunnel tests to demonstrate the overshoot that occurs near the wall in the velocity profile of a flow in a duct when the flow is subjected to oscillations in the axial pressure gradient.

4.9.2 Key equations

Although Richardson's annular effect is ordinarily beyond the scope of the first course in fluid mechanics, it represents a very practical use of experimental data that are obtainable from the study of boundary-layer flows in a duct.

Consider unsteady flow in a duct that is very long and in which one assumes that fully developed flow has been achieved. Let the duct be a pipe of circular cross section. One

assumes that the flow is entirely in the axial direction, and its velocity is only a function of two variables, the radial position, r , and the time, t . If one further assumes that the pipe is horizontal with internal radius r_0 and that the pressure gradient in the axial direction is $-\rho K \cos(\omega t)$, then, the solution of the thus-simplified Navier-Stokes equations for the velocity is given by the real part of

$$u = \frac{K}{i\omega} e^{i\omega t} \left[1 - \frac{J_0\left(r\sqrt{\frac{i\omega}{\nu}}\right)}{J_0\left(r_0\sqrt{\frac{i\omega}{\nu}}\right)} \right] \quad (24)$$

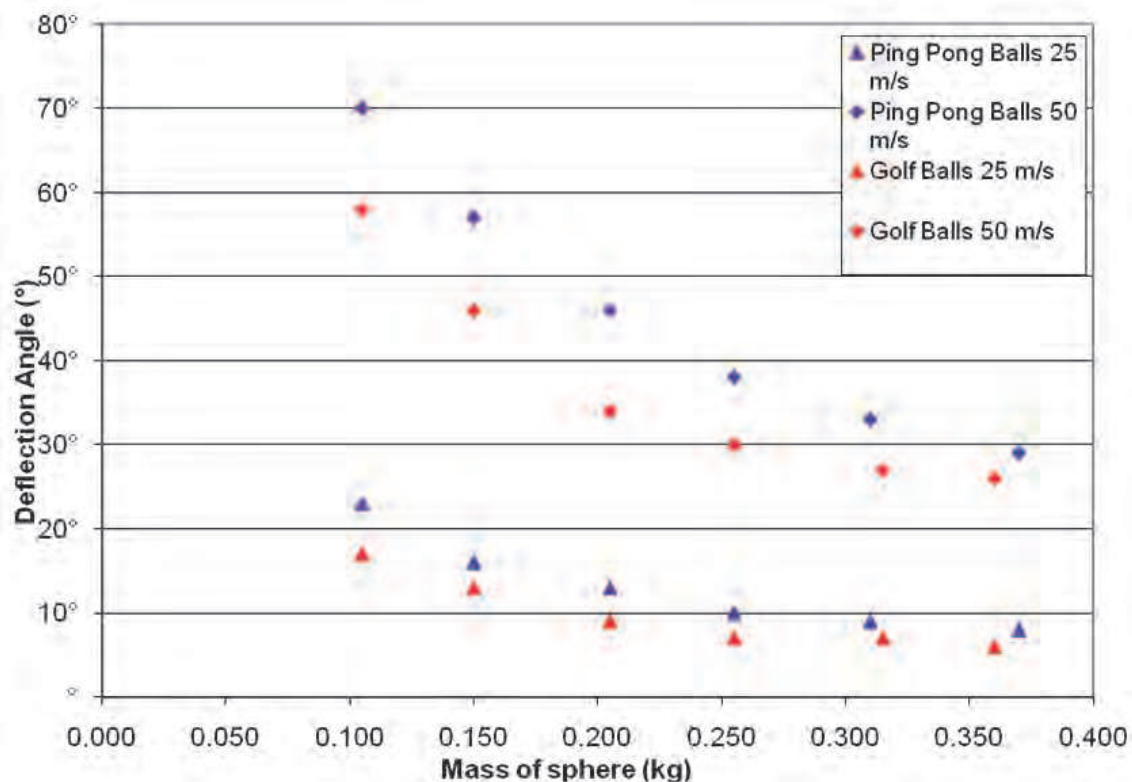


Fig. 17. Deflection angle of the pendulum in the test section vs. mass of the sphere.

Where J_0 denotes the Bessel function of the first kind and zero order, K is a constant, ρ is the mass density of the fluid and ω is the circular frequency of the oscillation.

One introduces non-dimensional quantities such that

$$r^* \equiv \frac{r}{r_0}; \omega^* \equiv \frac{\omega r_0^2}{\nu}; u^* \equiv \frac{u}{u_{max}} \quad (25)$$

Where u_{max} is the maximum centerline velocity for a steady Poiseuille flow in the same pipe that has a constant pressure gradient equal to $-\rho K$. It is known that oscillating flows of this type may become turbulent when ω^* exceeds 2000. For large values of ω^* a region of large velocity is established near the wall of the pipe and the mean square velocity is given by

$$\frac{\overline{u^2}}{K^2 / 2\omega^2} = 1 - \frac{2}{\sqrt{r^*}} e^{-B} \cos(B) + \frac{e^{-2B}}{r^*} \tag{26}$$

where

$$B = (1 - r^*) \sqrt{\frac{\omega^*}{2}} \tag{27}$$

When this equation is plotted as B vs. $\frac{\overline{u^2}}{K^2 / 2\omega^2}$, one observes that the velocity displays an overshoot near the wall, indicating that the maximum velocity occurs near the wall and not at the center of the pipe, as is the case for Poiseuille flow in a circular pipe. Such a plot is shown in Figure 18.

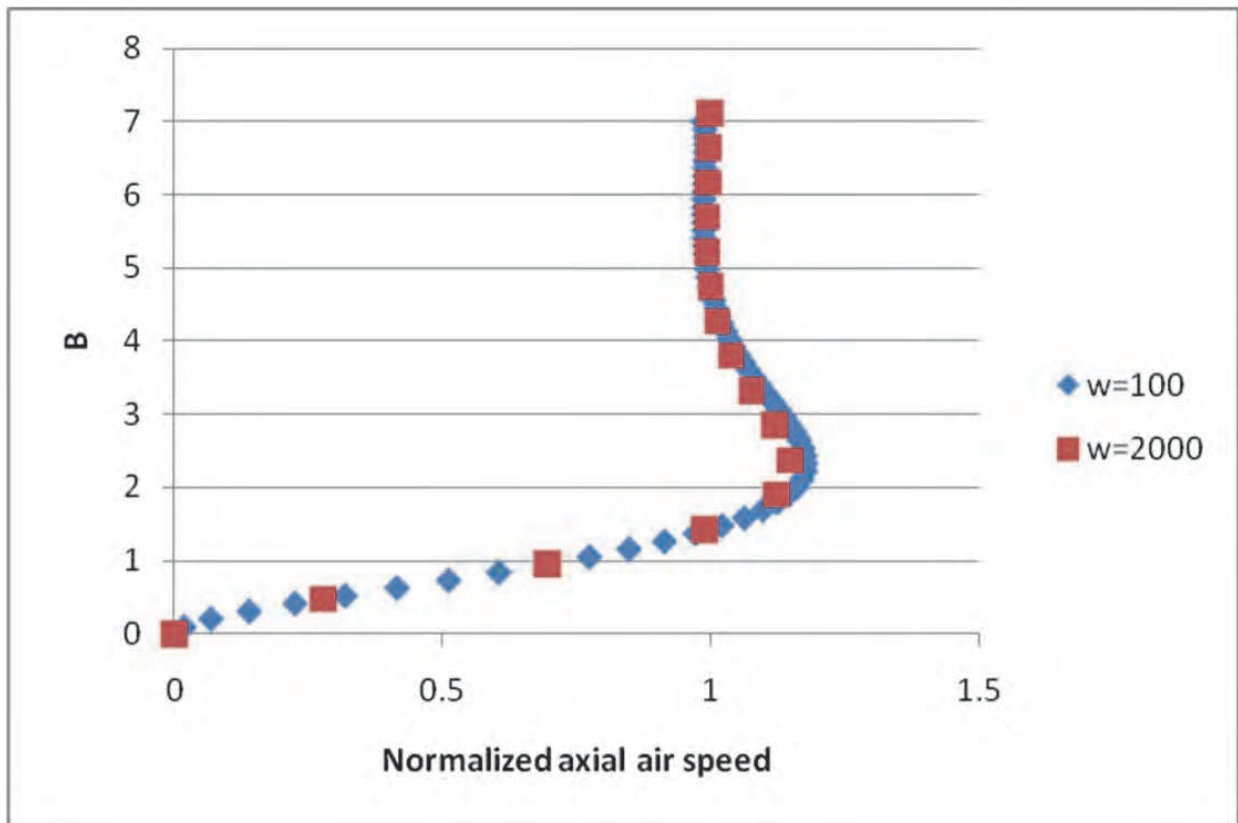


Fig. 18. Overshoot of velocity near the wall, known as Richardson’s annular effect

A similar phenomenon was observed in the velocity profile of flow in the wind tunnel that was shown in Figure 10.

4.9.3 Experimental procedure

One needs a close-up view of the plot of collected data near the maximum values achieved by the velocity. This can be achieved by zooming in on the velocity profile of the flow in the test section and by focusing of the velocity near the wall in Figure 10.

4.9.4 Experimental results

The graph in Figure 10 has been enlarged near the maximum values achieved by the velocity. The result is shown in Figure 19. The overshoot of the velocity near the wall, which is Richardson's annular effect, becomes plain and evident in that Figure.

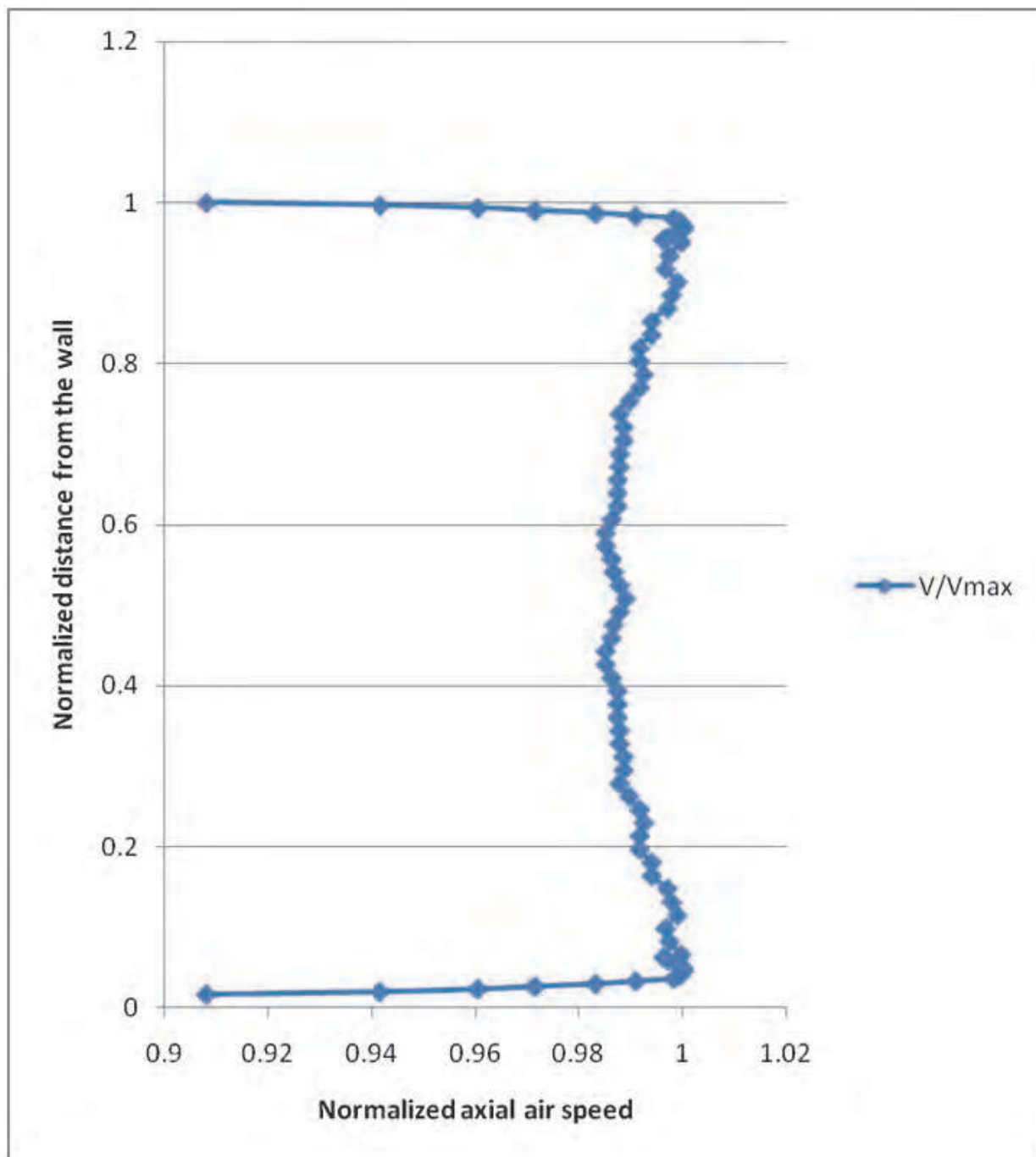


Fig. 19. Demonstration of Richardson's annular effect in the test section $\alpha \equiv (\omega / 2\nu)^{1/2}$.

A pulsating laminar flow of a viscous incompressible liquid in a rectangular duct of cross-sectional dimensions a and h was solved numerically (Yakhot et al., 1998,1999). Yakhot et al. performed calculations for low and high frequency regimes ($1 \leq \alpha h \leq 20$) in a rectangular

duct with different aspect ratios ($a/h = 1$ and 10). Their results clearly demonstrate the existence of Richardson's annular effect, Figure 20. The results in that Figure are very similar to those that were obtained from the wind tunnel and are shown in Figure 19.

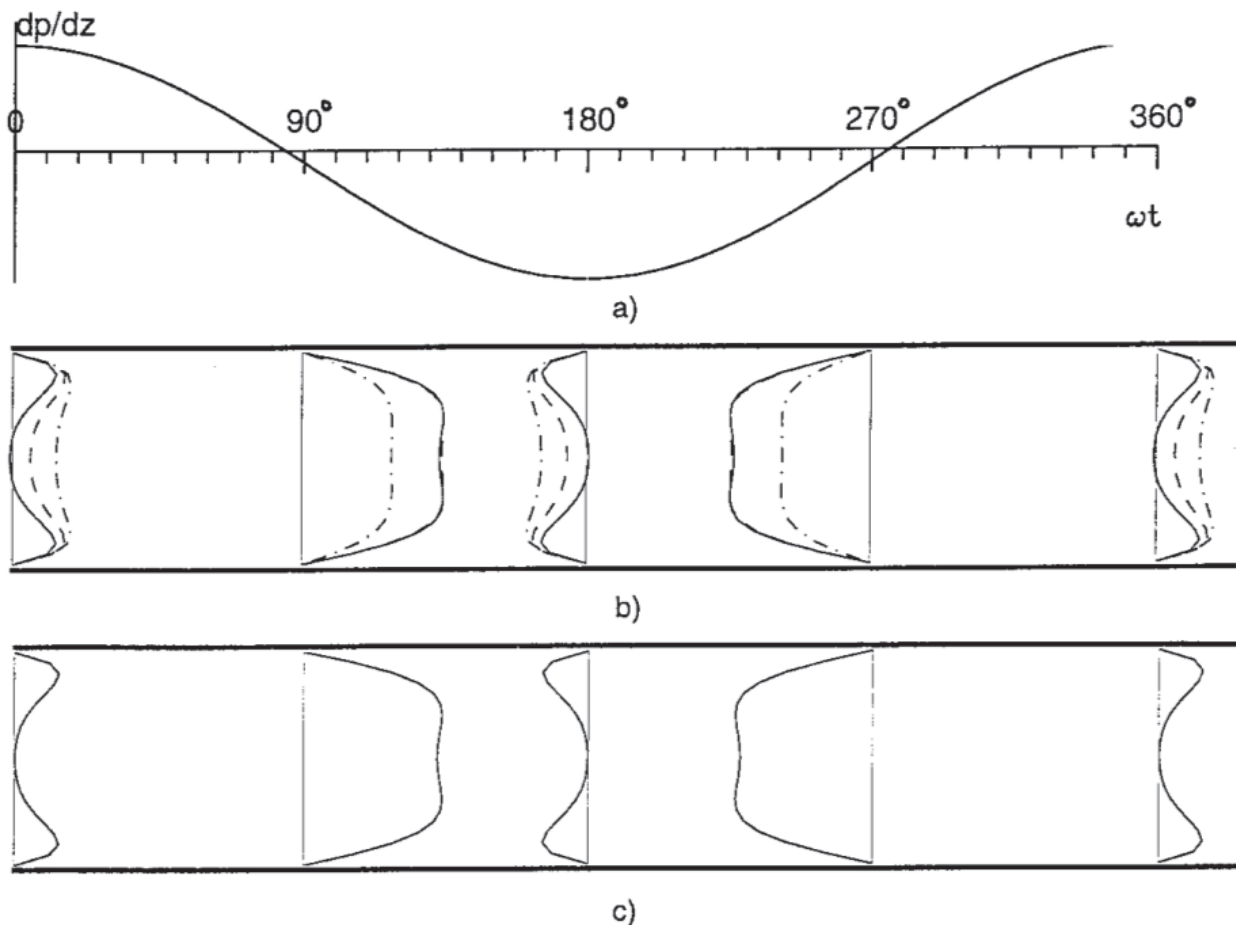


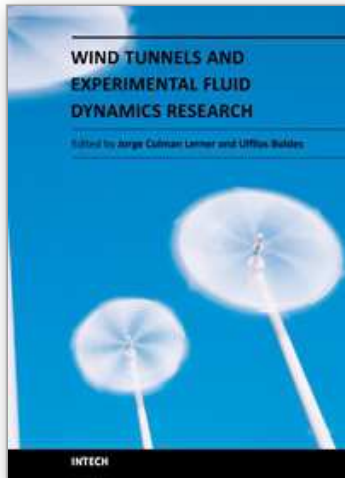
Fig. 20. Velocity profiles in pulsating flow at different instants of one period. (a) Pressure gradient variation with time. (b) Duct flow, $ah = 8$: solid line, $x/a = 0.5$; dashed, $x/a = 0.25$; dot-dashed, $x/a = 0.1$. (c) Flow between two parallel plates (Yakhot et al., 1999).

5. References

- Ernst, E. (1983). *The Undergraduate Engineering Laboratory*, Proceedings of an Engineering Foundation Conference, Edward W. Ernst, Editor, ISBN: 0939204215, New England College, Henniker, New Hampshire, July 1983
- Feisel, L., Rosa, A. (2005) The role of the engineering laboratory, *Journal of Engineering Education*, Vol. (January 2005), pp. (121-130), ISBN 0-309-08291-9.
- Njock Libii, J. (2006) Design of an experiment to test the effect of dimples on the magnitude of the drag force on a golf ball. *World Transactions on Engineering and Technology Education (WTE&TE)*, Vol.5, No. 3, (December 2006), pp. (477-480), ISSN 1446-2257
- Njock Libii, J. (2007) Dimples and drag: Experimental demonstration of the aerodynamics of golf balls. *American Journal of Physics*, Vol. 75, No. 8, (August 2007), pp. (764 -767), ISSN 0002-9505.

- Njock Libii, J. (2010) Laboratory exercises to study viscous boundary layers in the test section of an open-circuit wind tunnel, *World Transactions on Engineering and Technology Education(WTE&TE)*, Vol. 8, No. 1, (March 2010), pp. (91-97), ISSN 1446-2257.
- Njock Libii, J. (2010) Using wind tunnel tests to study pressure distributions around a bluff body: the case of a circular cylinder, *World Transactions on Engineering and Technology Education(WTE&TE)*, Vol. 8, No. 3, (December 2010), pp.(361-367), ISSN 1446-2257
- Njock Libii, J. & Russell R. Tobias, R. (2006). Lifting Bodies, In: *USA in Space (Third Edition)*, Russell R. Tobias and David G. Fisher, pp. (744-748), Salem Press, ISBN: 1-58765-259-5, Pasadena, California
- Pritchard, P. (2011). *Fox and McDonald's Introduction to Fluid Mechanics* (Eighth edition), John Wiley & Sons, ISBN-13 9780470547557, ISBN-10 0470547553, New York, NY.
- Rutgers, <http://coewww.rutgers.edu/classes/mae/mae433/lab3.pdf>, n.d.
- Sonntag, R., Borgnakke, C., & Van Wylen, G. (1998). *Fundamentals of Thermodynamics* (Fifth Edition), John Wiley & Sons, Inc., ISBN 0-471-18361-X, New York, 1998.
- Yakhot, A., M. Arad, M., & Ben-Dor, G. (1998). Richardson's Annular Effect in Oscillating Laminar Duct Flows. *Journal of Fluids Engineering*, Vol. 120, 1, (March 1998) pp. (209-301), ISSN 0098-2202
- Yakhot, A., M. Arad, M., & Ben-Dor, G. (1999). Numerical investigation of a laminar pulsating flow in a rectangular duct. *International Journal For Numerical Methods In Fluids*, Vol. 29, (1999) , pp. (935-950), ISSN 0271-2091

IntechOpen



Wind Tunnels and Experimental Fluid Dynamics Research

Edited by Prof. Jorge Colman Lerner

ISBN 978-953-307-623-2

Hard cover, 709 pages

Publisher InTech

Published online 27, July, 2011

Published in print edition July, 2011

The book "Wind Tunnels and Experimental Fluid Dynamics Research" is comprised of 33 chapters divided in five sections. The first 12 chapters discuss wind tunnel facilities and experiments in incompressible flow, while the next seven chapters deal with building dynamics, flow control and fluid mechanics. Third section of the book is dedicated to chapters discussing aerodynamic field measurements and real full scale analysis (chapters 20-22). Chapters in the last two sections deal with turbulent structure analysis (chapters 23-25) and wind tunnels in compressible flow (chapters 26-33). Contributions from a large number of international experts make this publication a highly valuable resource in wind tunnels and fluid dynamics field of research.

How to reference

In order to correctly reference this scholarly work, feel free to copy and paste the following:

Josué Njock Libii (2011). Wind Tunnels in Engineering Education, Wind Tunnels and Experimental Fluid Dynamics Research, Prof. Jorge Colman Lerner (Ed.), ISBN: 978-953-307-623-2, InTech, Available from: <http://www.intechopen.com/books/wind-tunnels-and-experimental-fluid-dynamics-research/wind-tunnels-in-engineering-education>

INTECH
open science | open minds

InTech Europe

University Campus STeP Ri
Slavka Krautzeka 83/A
51000 Rijeka, Croatia
Phone: +385 (51) 770 447
Fax: +385 (51) 686 166
www.intechopen.com

InTech China

Unit 405, Office Block, Hotel Equatorial Shanghai
No.65, Yan An Road (West), Shanghai, 200040, China
中国上海市延安西路65号上海国际贵都大饭店办公楼405单元
Phone: +86-21-62489820
Fax: +86-21-62489821

© 2011 The Author(s). Licensee IntechOpen. This chapter is distributed under the terms of the [Creative Commons Attribution-NonCommercial-ShareAlike-3.0 License](#), which permits use, distribution and reproduction for non-commercial purposes, provided the original is properly cited and derivative works building on this content are distributed under the same license.

IntechOpen

IntechOpen